

Primary Crystallization Region of NaAl(MoO₄)₂, Cr³⁺ Doping, Crystal Growth, and Characterization

A. Peña, R. Solé, Jna. Gavaldà, J. Massons, F. Díaz, and M. Aguiló*

Física i Cristal·lografia de Materials (FiCMA), Universitat Rovira i Virgili, Campus Sescelades, c/Marcel·lí Domingo, s/n, 43007 Tarragona, Spain

Received September 13, 2005. Revised Manuscript Received November 23, 2005

The main aim of this study was to determine the primary crystallization region of NaAl(MoO₄)₂ (NAM) in its self-flux. We determined the saturation temperature isotherms of NAM and two neighboring phases, Na₂Mo₂O₇ and Al₂(MoO₄)₃, in the ternary system Na₂O–Al₂O₃–MoO₃. We have analyzed several growing conditions in an effort to optimize the quality of single crystals obtained by a top-seeded solution growth technique. In the present work, we studied the thermal behavior of undoped and Cr³⁺-doped crystal and found a reversible phase transition at about 780 K. We also studied the evolution of the cell parameters of NAM as a function of temperature between room temperature and 573 K, and the linear thermal expansion tensor was determined. Furthermore, we determined some optical properties, such as the transparency window of NaAl(MoO₄)₂ and NaAl_{0.99}Cr_{0.01}(MoO₄)₂, the UV cutoff for both materials, and the spectroscopic characterization of Cr³⁺ in this crystal.

Introduction

Tunable solid-state lasers are of interest in scientific research because of their applications in many scientific and technological fields, such as spectroscopy, communications, and medicine. In an effort to find new materials with applications as tunable lasers, we studied sodium aluminum double molybdate, NAM, which belongs to a family of materials with the general formula M⁺M³⁺(M⁶⁺O₄)₂, where M⁺ = Na, K, Rb, Cs; M³⁺ = Al, Cr, In, Sc, and M⁶⁺ = Mo, W. This family of materials, when doped with Cr³⁺, has been shown to have interesting properties in tunable laser applications.^{1–6}

NAM, which is isostructural to NaFe(MoO₄)₂ and NaCr(MoO₄)₂, crystallizes in the monoclinic space group C2/c, with *a* = 9.621(2) Å, *b* = 5.3390(1) Å, *c* = 13.146(3) Å, β = 90.01(3)°, and four formula units per unit cell (*Z* = 4).⁷ Mo and O atoms are in general positions, but Na and Al atoms are in special positions on a 2-fold rotation axis and an inversion center, respectively. When the compounds are doped with Cr³⁺, the Cr³⁺ replaces the Al³⁺ atoms at the inversion center.

To date, single crystals of NAM were grown by the thermal method developed by Klevtsov et al.,⁸ however, there

is a lack of information in the literature about optimum conditions for obtaining high-quality single crystals. The determination of the crystallization region of this crystal in the ternary system Na₂O–Al₂O₃–MoO₃ is very important for optimizing its growth conditions to obtain high-quality single crystals by a top-seeded solution growth–slow cooling method.

In previous studies on NAM, done in the 1970s, it was said that this material had two phase transitions, one at 703 K, which was revealed when observing the domain structure, and the second one close 913 K, which was said to be the transition to the trigonal phase.^{9,10} In a recent study of the NAM phase transitions that used Raman scattering under high pressures, two pressure-induced phase transitions were found at about 1.1 and 3.3 GPa.¹¹ We chose X-ray diffraction and differential thermal analysis to try to find phase transitions in NAM and NAM:Cr³⁺ samples.

Furthermore, we studied, in the present work, the evolution of the NAM cell parameters with the temperature and have determined its linear thermal expansion tensor.

Finally, we determined the transparency window of the undoped and Cr³⁺-doped matrix. Room-temperature spectroscopy of Cr³⁺, optical absorption, and emission were also carried out. It has to be noticed that the optical absorption and emission results, obtained in this study, match those obtained in a previous optical study of this crystal.¹²

* To whom correspondence should be addressed. E-mail: magdalena.aguiló@urv.net.

- (1) Kaminskii, A. A. *Laser Crystals*; Academy of Sciences, Nauk SSSR: Moscow, 1975.
- (2) Kaminskii, A. A.; Sarkisov, S. E.; Bohm, J.; Reiche, P.; Schultze, D.; Vecker, R. *Phys. Solid State* **1977**, *43*, 71.
- (3) Lazoryak, B. I.; Efremov, V. A. *Sov. Phys. Crystallogr.* **1986**, *31*, 138.
- (4) Huber, G.; Lenth, W.; Lieberts, J.; Lutz, F. *J. Lumin.* **1978**, *16*, 353.
- (5) Voda, M.; Balda, R.; Sez de Ocanz, I.; Lacha, L. M.; Illarramendi, M. A.; Fernandez, J. J. *Alloys Compd.* **1998**, *214*, 275.
- (6) Hanuza, J.; Maczka, M.; Hermanowicz, K.; Andruszkiewicz, M.; Pietraszko, A.; Strek, W.; Derén, P. *J. Solid State Chem.* **1993**, *105*, 49.
- (7) Kolitsch, U.; Maczka, M.; Hanuza, J. *Acta Crystallogr.* **2003**, *E59*, i10.

- (8) Klevtsov, P. V.; Kozeeva, L. P.; Klevtsova, R. F. *Zh. Neorg. Khim.* **1975**, *20*, 2999.
- (9) Dudnik, E. F.; Sinyakov, E. V.; Stolpakova, T. M.; Dovchenko, G. V. *Fiz. Tverd. Tela* **1976**, *5*, 1419.
- (10) Otko, A. I.; Nesterenko, N. M.; Povstyanyi, L. V. *Phys. Status Solidi A* **1978**, *46*, 577.
- (11) Paraguassu, W.; Souza Filho, A. G.; Maczka, M.; Freire, P. T. C.; Melo, F. E. A.; Mendes Filho, J.; Hanuza, J. *J. Phys.: Condens. Matter* **2004**, *16*, 5151.
- (12) Hermanowicz, K.; Maczka, M.; Derén, P. J.; Hanuza, J.; Strek, W.; Drulis, H. *J. Lumin.* **2001**, *92*, 151.

Experimental Section

NAM Crystallization Region. We have studied different solution compositions to determine the primary crystallization region and crystallization temperatures of the NAM phase in the ternary system Na₂O–Al₂O₃–MoO₃. The experiments were carried out in a vertical tubular furnace, and the temperature was controlled by a Eurotherm 818P controller-programmer. We used 25 cm³ platinum crucibles filled with 13–20 g of solution to carry out the experiments. The initial reagents were Na₂CO₃, Al₂O₃, and MoO₃ that were mixed in the desired ratios. The mixed reagents were decomposed by heating them until there was a total bubbling of CO₂. We then homogenized the solution by keeping the temperature constant at about 300 K above the expected saturation temperature. It has to be mentioned that working at temperatures around 1350 K means having a high level of MoO₃ evaporation, so there could be some changes in the solution composition. The axial temperature difference between the surface and the bottom of the solution was about 5 K, with the bottom being hotter than the surface. After the solution reached homogenization, the temperature was lowered by 10 K every 30 min until crystals appeared on a platinum wire immersed in the solution. The saturation temperature was then accurately determined by observing the growth and dissolution of the crystals as a function of the temperature. After the determination of the saturation temperature, we decreased the solution temperature by 10 K at a rate of 0.5 K/h in order to grow the crystals.

The crystals obtained were first observed with an optical microscope and then identified by X-ray powder diffraction analysis. After studying about 30 different compositions, we obtained the crystallization region and saturation temperatures of NAM in the self-flux.

X-ray Powder Diffraction. We used the X-ray powder diffraction technique to identify NAM and neighboring phases of the crystallization region determined. The equipment used to identify the crystalline powder samples was a Siemens D5000 powder diffractometer in a θ – θ configuration using the Bragg–Brentano geometry.

To study the evolution of the NAM crystal cell parameters with the temperature and NAM's linear thermal expansion, we used the same equipment, but in that case added a high-temperature chamber (Anton-Paar HTK10 platinum ribbon heating stage). The chosen range for carrying out the measurements was 298–973 K, and the X-ray powder diffraction patterns were recorded using a scintillation detector, with $2\theta = 10$ – 70° , step size = 0.03° , and step time = 5 s. To refine the cell parameters obtained in all the diffraction data collected at 298, 32, 373, 473, and 573 K, we used the FULLPROF program¹³ and the Rietveld method.¹⁴ As the starting model for the calculations, we used the coordinates of the atoms in NAM that appeared in a previous paper.⁷ The X-ray powder diffraction data recorded at 673, 773, 873, and 973 K gave us additional information about the crystalline structure of this material with the temperature.

To determine the phase transitions of NAM and NAM:Cr³⁺, we heated and cooled the sample using the same equipment but adding a Braun position sensitive detector (PSD). The X-ray powder diffraction patterns were recorded at $2\theta = 10$ – 70° , and the time used to measure each degree was 10 s. To study phase transitions, we recorded several diffraction patterns: the first at room temperature, the next at 650 K, then one every 50 K up to 950 K. The

cooling was then performed at the same rate and temperature intervals.

Differential Thermal Analysis (DTA) Measurements. Prior to studying phase transitions of NAM with X-ray powder diffraction, we analyzed them by DTA measurements. We used a TA Instruments simultaneous differential techniques instrument SDT 2960. We used less than 13 mg of sample placed in a platinum pan, and as a reference material we used close 13 mg of Al₂O₃. The experiment was performed using Ar as a purge gas with a flow of 90 cm³/min and a heating rate of 10 K/min between room temperature and 1050 K.

Top-Seeded Solution Growth. We wanted to obtain NAM:Cr³⁺ crystals of a suitable size and high enough quality for physical characterization and to further evaluate optical applications of this new material. Therefore, we carried out several growth experiments by the top-seeded solution growth–slow cooling (TSSG–SC) method. We used the same equipment as that used in the determination of the crystallization region, a vertical tubular furnace controlled by a Eurotherm 818P controller-programmer. Details about the experimental setup and the TSSG–SC methodology were published elsewhere.¹⁵

To carry out the crystal growth, we chose an initial molar composition of Na₂O–Al₂O₃–MoO₃ placed in the crystallization region to study the growth parameters and the doping with Cr³⁺. The solutions were prepared in conical platinum crucibles of 25 cm³ by mixing the appropriate amounts of the initial reagents, Na₂CO₃, Al₂O₃, and MoO₃, to obtain the desired molar composition. The axial temperature gradient was between 6.6 and 0.4 K/cm, with the bottom of the crucible being hotter than the surface. We then homogenized the solution, as has been explained in the study of the crystallization region. We used small seeds with the *b* crystallographic direction perpendicular to the surface of the solution and located at the center of the solution surface. To determine the saturation temperature, we accurately observed the growth and dissolution processes of the seed in contact with the surface of the solution, keeping the rotation velocity of the seed constant. The reagent used to dope NAM was Cr₂O₃. We studied different concentrations of Cr₂O₃, substituting Al₂O₃ in the initial solution, and determined suitable values for the crystal growth parameters.

Dopant Concentration Analyses. Some of the obtained NAM:Cr³⁺ crystals, with different Cr³⁺ concentrations, were analyzed by electron probe microanalysis (EPMA) to determine the concentration of Cr³⁺. A Cameca SX50 microprobe analyzer, in the wavelength dispersive mode operating at a 20 kV accelerating voltage and 15 nA beam current for all the components, was used to take the measurements. The crystals used were included in cylinders of resin, and the surfaces were polished with diamond powders of 1 μ m grain size. After that, the samples were recovered with the same thickness as the samples used for standards.

Optical Characterization. We measured the transmission in samples of NAM and NAM:Cr³⁺ crystals and the absorption and fluorescence emission in a NAM:Cr³⁺ crystal. The transmission was measured using a Varian Cary scan spectrophotometer in the 300–3000 nm range and a FT-IR-680 Plus Fourier transform infrared spectrometer in the 3000–8000 nm range. The optical absorption bands of Cr³⁺ in NAM at room temperature were also measured by the Varian Cary scan spectrophotometer, and the emission was measured with a BMI optical parametric oscillator (OPO) pumped by the third harmonic of a seeded BMI SAGA Q-switch YAG:Nd laser. Fluorescence was dispersed through a HR460 Jobin Yvon-Spex monochromator and detected by a

(13) Rodríguez-Carvajal, J. *Short Reference Guide for the Computer Program FULLPROF*; Laboratoire León Brillouin, CEA-CNRS: Saclay, France, 1998.

(14) Young, R. A. *The Rietveld Method*; Oxford Science Publication, International Union of Crystallography: New York, 1995.

(15) Solé, R.; Nikolov, V.; Ruiz, X.; Gavaldà, J.; Solans, X.; Aguiló, M.; Díaz, F. *J. Cryst. Growth* **1996**, *169* (3), 600.

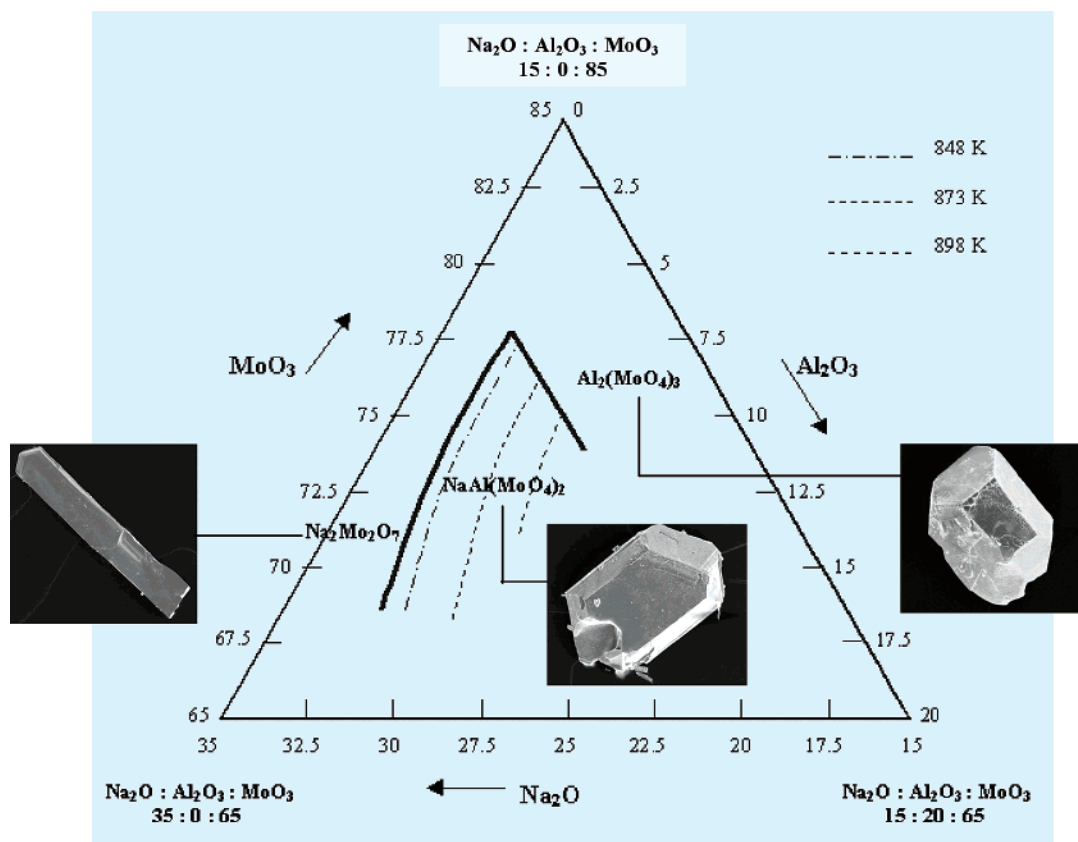


Figure 1. Crystallization region of NAM and saturation temperatures in the ternary system $\text{Na}_2\text{O}-\text{Al}_2\text{O}_3-\text{MoO}_3$ (mol %). SEM images of NAM and neighboring phases.

Hamamatsu R928 photomultiplier connected to an EG&G 7265DSP lock-in amplifier.

Results and Discussion

NAM Crystallization Region. After studying about 30 different compositions, we obtained the crystallization region and saturation temperatures of NAM in the ternary system $\text{Na}_2\text{O}-\text{Al}_2\text{O}_3-\text{MoO}_3$. Figure 1 shows the crystallization region of NAM in its self-flux, the saturation temperature isotherms, and two neighboring phases. SEM images of NAM and neighboring phases are also shown in this figure.

The limitation of working with temperatures below 1350 K has restricted the studied area. It has been impossible to work with Al_2O_3 concentrations above 5.5 mol % because of the high evaporation levels of MoO_3 when the temperature is increased to try to homogenize the solution. So the NAM phase appears with solutions containing Al_2O_3 concentrations greater than 2.3 mol % and MoO_3 between 68 and 78 mol %. Its saturation temperature isotherms range from less than 850 K to more than 1000 K, and the temperature increases as the $\text{Na}_2\text{O}:\text{Al}_2\text{O}_3$ molar ratio decreases from 90:10 to 80:20.

The neighboring phases identified in the crystallization region determined are $\text{Na}_2\text{Mo}_2\text{O}_7$ ¹⁶ and $\text{Al}_2(\text{MoO}_4)_3$.¹⁷ The former appeared for concentrations of Al_2O_3 below 2.3 mol %, and $\text{Al}_2(\text{MoO}_4)_3$ appeared for solutions with concentra-

tions of MoO_3 above 75 mol % and Na_2O below 20 mol %. The crystals obtained of $\text{Na}_2\text{Mo}_2\text{O}_7$ were colorless and had a needle shape, and those of $\text{Al}_2(\text{MoO}_4)_3$ had a pale yellow color.

Crystal Morphology of NAM. To describe the morphology of the crystals, we observed by scanning electron microscopy (SEM) many small crystals of NAM grown by spontaneous crystallization on a Pt wire (Figure 2a). These crystals showed a pseudohexagonal shape, as can be seen in Figure 2a. The theoretical habit drawn with the Shape software,¹⁸ in which most faces are hexagonal or trapezoidal, is shown in Figure 2b. The habit of crystals grown was formed by the crystalline forms $\{001\}$, $\{100\}$, $\{110\}$, $\{\bar{1}01\}$, $\{101\}$, $\{112\}$, and $\{11\bar{2}\}$.

In the visualization of the crystals, we saw exfoliation planes, and by using X-ray diffraction analysis, we determined that these exfoliation planes are perpendicular to the $[001]$ direction.

$\text{NAM}:\text{Cr}^{3+}$ crystals showed the same morphology as that of NAM and also had in the same cleavage plane.

Linear Thermal Expansion Tensor. Knowing how the behavior of a laser material changes with increases in temperature is important in determining the thermal expansion tensor, because pumping involves a change in the temperature inside the crystal.

To study the evolution of the cell parameters with the temperature, we used X-ray powder diffraction between 298

(16) Seleborg, M. *Acta Chem. Scand.* **1967**, *21*, 499.

(17) Harrisson, W. T. A.; Cheetham, A. K.; Faber, J. J. *Solid State Chem.* **1988**, *76*, 328.

(18) Dowty, E. *Shape for Windows*, version 5.0.1; Shape Software: Kingsport, TN, 1995.

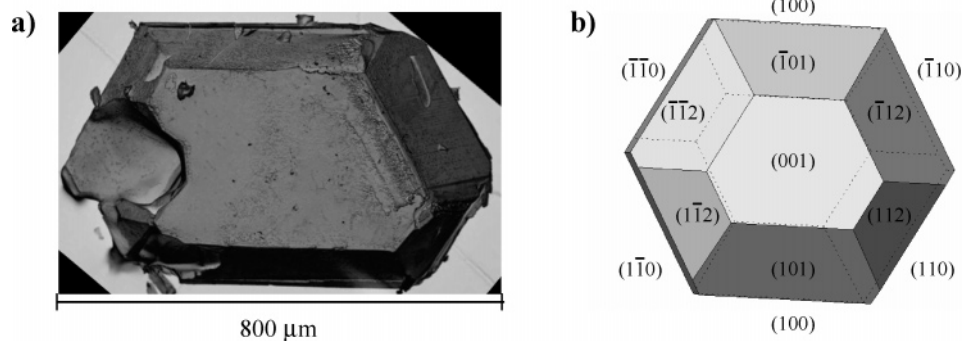


Figure 2. (a) NAM small single crystal grown by spontaneous crystallization on a Pt wire. (b) Scheme of the crystal morphology.

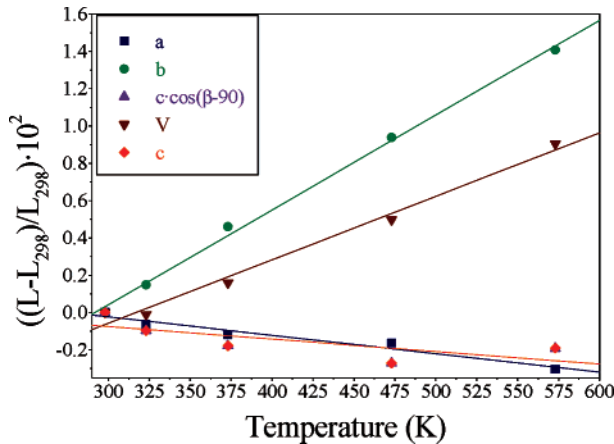


Figure 3. Thermal evolution of the cell parameters and unit cell volume of NaAl(MoO₄)₂.

and 573 K. To refine these cell parameters, obtained previously using X-ray powder diffraction, we used the FULLPROF program¹³ and the Rietveld method.¹⁴ In Figure 3, it is shown the linear relationship between $\Delta L/L$ and temperature, where L is a cell parameter at room temperature and ΔL is the change in this parameter when there is a change in the temperature, ΔT . Cell volume and b increased with temperature, and a , c , and $c \cdot \cos(\beta - 90)$ decreased as temperature increased.

The linear thermal expansion defined as $\alpha = (1/L)(\Delta L/\Delta T)$ can be calculated from the slope of the linear fitting for each unit cell parameter, as shown in Figure 3. Here, there is the linear thermal expansion tensor in the crystallophysical system $X_1||\bar{a}$, $X_2||\bar{b}$, $X_3||\bar{c}^*$

$$\alpha_{ij} = \begin{pmatrix} -10 & 0 & 5 \times 10^{-3} \\ 0 & 51 & 0 \\ 5 \times 10^{-3} & 0 & -7 \end{pmatrix} \times 10^{-6} \text{ K}^{-1}$$

Although we are working with a monoclinic system, the fact that $\beta = 90.01(3)^\circ$ means the angle between \bar{c} and \bar{c}^* is 0.01, α_c and $\alpha_{c^*} = \alpha_{33}$ have almost the same value, and α_{13} is 4 orders of magnitude smaller. So the diagonalized linear thermal expansion tensor is

$$\alpha'_{ij} = \begin{pmatrix} -10 & 0 & 0 \\ 0 & 51 & 0 \\ 0 & 0 & -7 \end{pmatrix} \times 10^{-6} \text{ K}^{-1}$$

That means that the crystallographic system (a , b , c), the crystallophysical system (X_1 , X_2 , X_3), and the principal axis

system (X_1' , X_2' , X_3') are roughly parallel. In that case, we can write that $X_1||a||X_1'$, $X_2||b||X_2'$, and $X_3||c^*||X_3'$.

The NAM crystal presents a high thermal anisotropy. The expansion coefficient in the b direction is about six times bigger than the values shown in the a - c plane. As a consequence of this thermal behavior and in order to avoid the generation of cracks in crystals, it is convenient to establish very low rates when the crystals are exposed to the heating or cooling processes.

TSSG of Undoped and Cr³⁺-Doped NAM. In all the experiments done to obtain single crystals of NAM and NAM:Cr³⁺ by TSSG, we used seeds with the [010] direction perpendicular to the surface of the solution and placed in the center of the crucible. It is noteworthy that we have chosen this seed orientation because of the existence of cleavage planes perpendicular to the [001] direction, and the dimension of the grown crystals along the [010] direction is typically double the length along the [100] direction.

We chose the molar composition Na₂O:Al₂O₃:MoO₃ = 21.600:2.400:76.000 and prepared 25 g of solution to carry out this study. As can be seen in Figure 1, this solution corresponds to a point placed in the left-hand side of the crystallization region. At first, we need a precise determination of the saturation temperature, T_s . Studying the processes of growth and dissolution of a single-crystal seed of NAM in touch with this solution, we determined T_s to be 858 K; at this temperature, the slow cooling process can start. We tried to optimize growth conditions with undoped crystals. Taking into account the cooling rate, after a preliminary test that involved observing the inclusion concentration in the nucleated crystals grown on a Pt disk, we conclude that the value of 0.1 K/h is a reasonable cooling rate value, with a good compromise between the quality of the crystals and the time of growth. We noticed that, after many experiments, the rotation velocity of the seed in the range of 4 to 80 rpm has no detectable effect on the quality of the crystals obtained, as a consequence of the low viscosity of the solution. Consequently, we fixed its value at 60 rpm for all the experiments. It was accidentally detected that the axial temperature gradient has a relevant effect on the quality of the grown crystals. To confirm this effect, we performed a set of experiments that involved varying the axial position of the crucible in the vertical tube of the furnace and achieving a variation in temperature difference between the bottom of the crucible and the surface of the solution. The range of temperature gradients studied was $0.4 \text{ K/cm} \leq \Delta T/H$

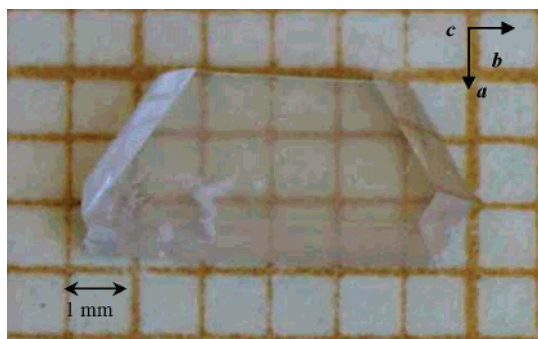


Figure 4. $\text{NaAl}_{0.99}\text{Cr}_{0.01}(\text{MoO}_4)_2$ single crystal grown by TSSG.

≤ 6.6 K/cm, where H is the height of the solution. The best conditions of growth, measured in terms of the inclusion concentration in the crystals, were obtained with $\Delta T/H = 0.4$ K/cm. It was not possible to reduce this temperature gradient, because with lower values the nucleation appears in others points of the solution.

After this preliminary study of NAM crystal growth, we focused all of our efforts on obtaining the optimal conditions for growing high-quality Cr^{3+} -doped single crystals. The initial composition of the solution from which we obtained the first results was $\text{Na}_2\text{O}:\text{Al}_2\text{O}_3:\text{Cr}_2\text{O}_3:\text{MoO}_3 = 21.600:2.388:0.012:76.000$ (mol %), and the solution weighed 25 g. The saturation temperature of the new solution was determined to be 887 K. We kept the optimal growth conditions found for NAM crystals. We defined 12 K as the cooling range established from the saturation temperature and 0.1 K/h as the cooling rate. Dark green colored polycrystalline samples have been obtained. The chemical composition measured by EPMA was $\text{NaAl}_{0.98}\text{Cr}_{0.02}(\text{MoO}_4)_2$, which corresponds to a Cr^{3+} concentration of 9.9×10^{19}

atoms/cm³. We noticed the host could easily incorporate Cr^{3+} into the Al^{3+} positions. The distribution coefficient, defined as $K_{\text{Cr}^{3+}} = ([\text{Cr}^{3+}]/([\text{Cr}^{3+}] + [\text{Al}^{3+}]))_{\text{crystal}}/([\text{Cr}^{3+}]/([\text{Cr}^{3+}] + [\text{Al}^{3+}]))_{\text{solution}}$, is about 3. This value being significantly higher than the unit indicates the capability of the host to incorporate Cr^{3+} in the Al^{3+} sites. Although the distribution coefficient was greater than unity, nonsignificant changes in the solution composition were expected because the size of the doped crystals grown in this work was very small in relation to the solution volume. After three experiments we could not obtain a single crystal; in all cases, the samples show a relevant concentration of inclusions, cracks, and others macroscopic defects, which is far from the desired optical quality of the material. Consequently, we decided to grow samples with a lower Cr^{3+} concentration.

We moved the composition to $\text{Na}_2\text{O}:\text{Al}_2\text{O}_3:\text{Cr}_2\text{O}_3:\text{MoO}_3 = 21.600:2.395:0.005:76.000$ and prepared 25 g of the solution. The saturation temperature of the new solution is 871 K. We kept the conditions of the previous crystal growth experiment, and after 5 days an inclusion-free and slightly green-colored single crystal was obtained. As can be seen in Figure 4, the grown crystal is plate shaped with about $3 \times 6 \times 1.5$ mm³ for the dimensions and 0.38 g for the weight. The chemical composition of the crystal, $\text{NaAl}_{0.99}\text{Cr}_{0.01}(\text{MoO}_4)_2$, was measured by EPMA, which corresponds to a Cr^{3+} concentration of 3.9×10^{19} atoms/cm³.

Phase Transitions. To study how NAM evolved with increasing temperature, as has been said before, we used differential thermal analysis (DTA) and the X-ray powder diffraction technique in parallel.

The data collected by DTA between 400 and 1050 K for the NAM and $\text{NaAl}_{0.98}\text{Cr}_{0.02}(\text{MoO}_4)_2$ samples showed us two

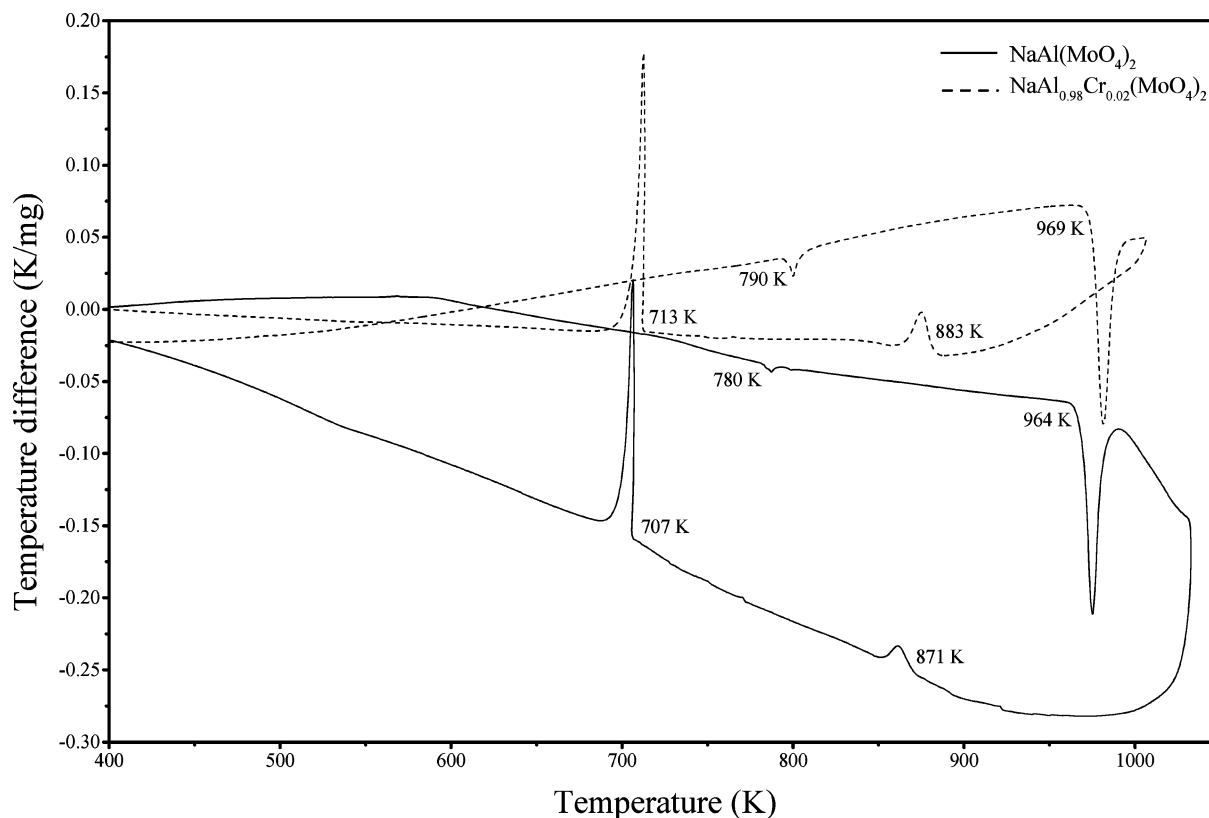


Figure 5. Differential thermal analysis (DTA) thermogram of $\text{NaAl}(\text{MoO}_4)_2$ and $\text{NaAl}_{0.98}\text{Cr}_{0.02}(\text{MoO}_4)_2$ in the 400–1050 K temperature range.

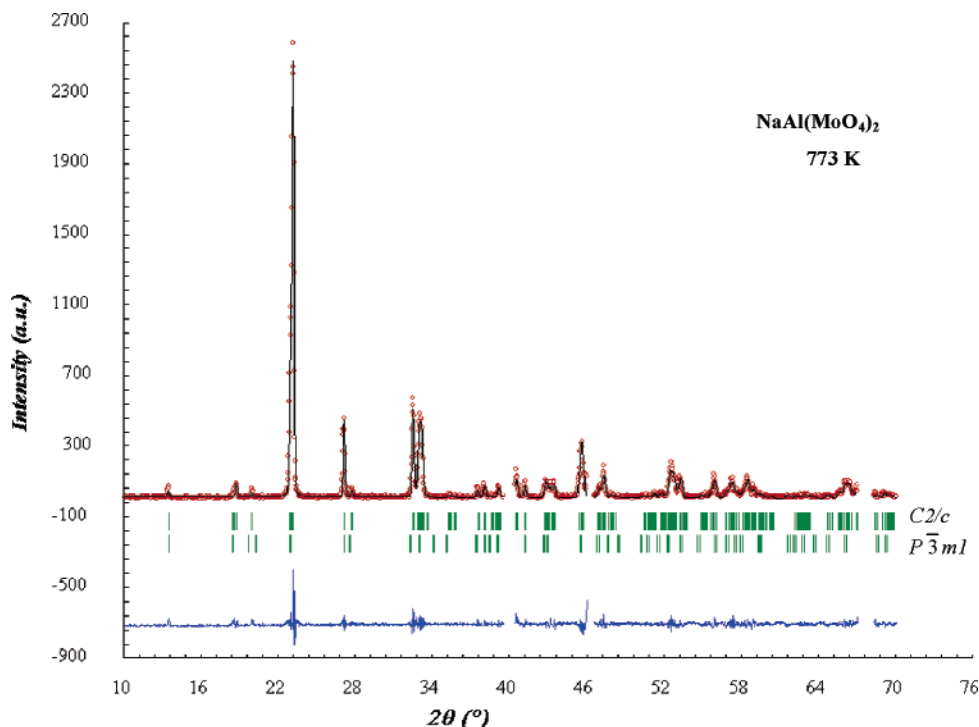


Figure 6. Refined X-ray diffraction pattern of $\text{NaAl}(\text{MoO}_4)_2$ showing the observed (points), calculated (full line), and difference (bottom) Rietveld profiles at 750 K and the reflection patterns of the monoclinic and trigonal phases.

endothermic peaks, as can be seen in Figure 5. The first, which appeared at 780 K for NAM and about 10 K above that for $\text{NaAl}_{0.98}\text{Cr}_{0.02}(\text{MoO}_4)_2$, could be due to a phase transition, but this temperature did not match with the temperature reported in the literature.^{9,10} We think there could be a phase transition at this temperature between the $C2/c$ monoclinic phase and the $P\bar{3}m1$ trigonal phase. The second endothermic peak, at a temperature of 964 K for NAM and 5 K above that for $\text{NaAl}_{0.98}\text{Cr}_{0.02}(\text{MoO}_4)_2$, corresponds to the melting of the material. While cooling the sample we also found two peaks, but because of the thermal hysteresis, both peaks appeared about 80 K below the temperature they appeared at in the heating rate plot. The first peak of the cooling rate plot, at 871 K in NAM and 883 K in $\text{NaAl}_{0.98}\text{Cr}_{0.02}(\text{MoO}_4)_2$, could be due to the crystallization of the trigonal phase, and the second one, at 707 K in NAM and 713 K in $\text{NaAl}_{0.98}\text{Cr}_{0.02}(\text{MoO}_4)_2$, is the phase transition of the monoclinic phase; therefore, the phase transition found is reversible. Nevertheless, the corresponding peaks in the heating and cooling processes in the DTA have different morphologies.

To obtain complementary information, we used the X-ray powder diffraction technique. First, the recorded X-ray powder diffraction patterns, with the conditions explained in the Experimental Section, were refined with the FULL-PROF program, and at temperatures higher than 750 K, the RF-factor and Bragg R-factor were better if we considered that two phases were present. Thus, the $C2/c$ phase did not disappear, but $P\bar{3}m1$ began to appear; therefore, above 780 K there were two phases. But we could not confirm that this statement is true because almost all the $P\bar{3}m1$ reflections match with the $C2/c$ reflections, as is shown in Figure 6.

Second, we have recorded the evolution of the material with temperature using X-ray powder diffraction, in parallel

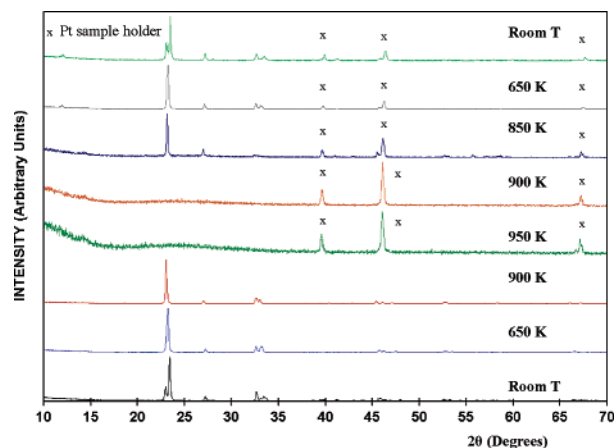


Figure 7. X-ray powder diffraction patterns recorded in the room temperature to 950 K range, in heating and cooling processes.

with the DTA measurements, as shown in Figure 7, where we have selected some patterns of the analysis. In the heating zone, the double principal peak at room temperature becomes a single peak at temperatures of 650 K and higher. At 950 K, the sample melted and all the peaks disappeared, except the one corresponding to the sample holder. In the cooling zone, in the range from 850 to 650 K, we observed the same patterns as in the heating process; at room temperature, the pattern obtained overlaps its corresponding pattern from the beginning of the process. In the cooling process, the intensity obtained is lower in every case.

In this way, the DTA and the X-ray powder diffraction studies agree and allow us to conclude that the transition phase is reversible.

Optical Absorption and Fluorescence Emission of $\text{NaAl}(\text{MoO}_4)_2$ and $\text{NaAl}_{0.99}\text{Cr}_{0.01}(\text{MoO}_4)_2$. We studied the transparency window of $\text{NaAl}(\text{MoO}_4)_2$ and $\text{NaAl}_{0.99}\text{Cr}_{0.01}(\text{MoO}_4)_2$. As shown in Figure 8, the transparency window is slightly wider in the doped

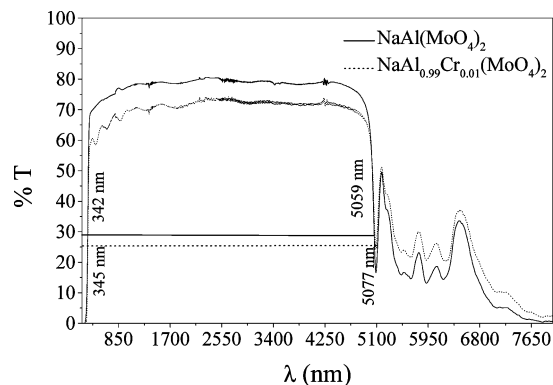


Figure 8. Transparency window of $\text{NaAl}(\text{MoO}_4)_2$ (solid line) and $\text{NaAl}_{0.99}\text{Cr}_{0.01}(\text{MoO}_4)_2$ (dotted line).

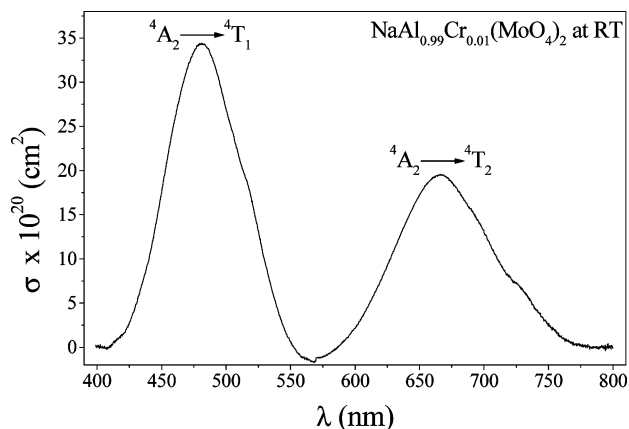


Figure 9. Room-temperature optical absorption of Cr^{3+} in $\text{NaAl}_{0.99}\text{Cr}_{0.01}(\text{MoO}_4)_2$.

crystal. In the case of $\text{NaAl}(\text{MoO}_4)_2$, the UV cutoff wavelength is 342 nm and the IR cutoff wavelength is 5059 nm; the corresponding values for $\text{NaAl}_{0.99}\text{Cr}_{0.01}(\text{MoO}_4)_2$ are 345 and 5077 nm, respectively. These cutoff wavelengths are determined as the value obtained when the transmission decays by a factor of $1/e$. The bands between 5000 and 7000 nm are due to combinations of symmetric and asymmetric vibrational modes of MoO_4 ,¹⁹ and the UV cutoff is related to the electronic gap of the material. In this figure, it can be seen that the main difference between the two transmission spectra is the two absorption broad bands that appeared, due to the presence of Cr^{3+} , in the $\text{NAM}:\text{Cr}^{3+}$ spectrum. These two broad bands, also observed in Figure 9, are due to the optical absorption of Cr^{3+} . The first one, at 481 nm, is attributed to the ${}^4\text{A}_2 \rightarrow {}^4\text{T}_1$ transition, and the second one, at 664 nm, is due to the ${}^4\text{A}_2 \rightarrow {}^4\text{T}_2$ transition,²⁰ which is the reason for the green color of the crystal.

Cr^{3+} has been used as the active ion in many hosts to obtain laser tunability, which must be associated with a weak crystal field in the Cr^{3+} sites. The NAM structure generates

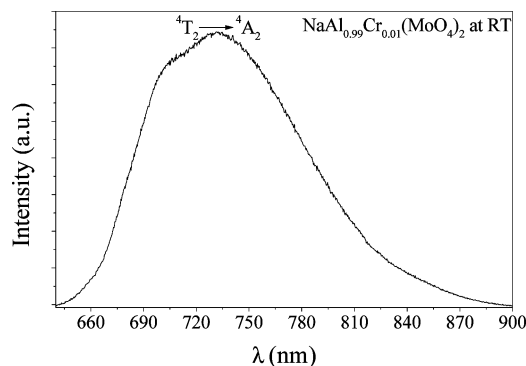


Figure 10. Room-temperature emission of Cr^{3+} in $\text{NaAl}_{0.99}\text{Cr}_{0.01}(\text{MoO}_4)_2$.

a low crystal field, and it induces tunability in the fluorescence emission channels. Figure 10 shows the RT emission broad band related to the ${}^4\text{T}_2 \rightarrow {}^4\text{A}_2$ spontaneous transition with a tunability ring of about 200 nm.

Conclusions

We obtained the crystallization region of NAM in the ternary system $\text{Na}_2\text{O}-\text{Al}_2\text{O}_3-\text{MoO}_3$. Its saturation temperatures are determined, and two neighboring phases are identified. As the percentage of Al_2O_3 in the solution increases, the temperature of homogenization and the evaporation of MoO_3 increase, so we work only with a percentage of Al_2O_3 below 5.5 mol %. To perform the crystal growth, we chose a point of the crystallization region obtained.

We determined the thermal expansion tensor of NAM, which shows a high thermal anisotropy, especially between the b direction and the $a-c$ plane.

We grew NAM and $\text{NAM}:\text{Cr}^{3+}$ single crystals by the top-seeded solution growth slow cooling method. The parameters of the growth were optimized to obtain single crystals of a suitable size and quality for further optical characterizations and to find out its possible applications.

In the thermal analysis of NAM and $\text{NAM}:\text{Cr}^{3+}$, we saw that there is a reversible phase transition from the monoclinic to the trigonal phase and that it appeared at a higher temperature when doped with Cr^{3+} .

Finally, we have determined the transparency window of NAM and detected that the Cr^{3+} doping increases it slightly. To confirm that $\text{NAM}:\text{Cr}^{3+}$ could have applications as a tunable solid-state laser, we measured the optical absorption and the emission at room temperature, and it shows a well-defined broad band of luminescence between 660 and 840 nm.

Acknowledgment. This work has been supported by the Spanish government under Projects MAT2002-04603-C05-03, MAT2005-06354-C03-02, and BES-2003-1694, and by the Generalitat de Catalunya under Projects 2001SGR317 and 2005SGR658.

CM052054J

(19) Maczka, M.; Hanuza, J.; Lutz, E. T. G.; van der Maas, J. H. J. *Solid State Chem.* **1999**, *145*, 751.

(20) Henderson, B.; Imbusch, G. F. *Optical Spectroscopy of Inorganic Solids*; Oxford University Press: New York, 1989.